

# Harmonized chronologies of a global late Quaternary pollen dataset (LegacyAge 1.0)

Chenzhi Li<sup>1,2</sup>, Alexander K. Postl<sup>1</sup>, Thomas Böhmer<sup>1</sup>, Xianyong Cao<sup>1,3</sup>, Andrew M. Dolman<sup>1</sup>,  
Ulrike Herzschuh<sup>1,2,4</sup>

<sup>1</sup> Alfred Wegener Institute, Helmholtz Centre for Polar and Marine Research, Polar Terrestrial Environmental Systems, Telegrafenberg A45, 14473 Potsdam, Germany

<sup>2</sup> Institute of Environmental Science and Geography, University of Potsdam, Karl-Liebknecht-Str. 24-25, 14476 Potsdam, Germany

<sup>3</sup> Alpine Paleoecology and Human Adaptation Group (ALPHA), State Key Laboratory of Tibetan Plateau Earth System, and Resources and Environment (TPESRE), Institute of Tibetan Plateau Research, Chinese Academy of Sciences, 100101 Beijing, China

<sup>4</sup> Institute of Biochemistry and Biology, University of Potsdam, Karl-Liebknecht-Str. 24-25, 14476 Potsdam, Germany

**Correspondence:** Ulrike Herzschuh (Ulrike.Herzschuh@awi.de)

**Abstract.** ~~We present a chronology framework named LegacyAge 1.0 containing harmonized chronologies for 2831 pollen records (downloaded from the Neotoma Paleoecology Database and the supplementary Asian datasets) together with their age control points and metadata in machine-readable data formats. Although numerous pollen records are available worldwide in various databases, their use for synthesis works is limited as the chronologies are, as yet, not harmonized globally, and temporal uncertainties are unknown. We present a chronology framework named LegacyAge 1.0 that includes harmonized chronologies of 2831 palynological records (out of 3471 available records), downloaded from the Neotoma Paleoecology Database (last access: April 2021) and 324 additional Asian records.~~ All chronologies use the Bayesian framework implemented in Bacon version 2.5.3. Optimal parameter settings of priors (accumulation.shape, memory.strength, memory.mean, accumulation.rate, thickness) were identified based on ~~information in the original publication previous experiences~~ or iteratively after preliminary model inspection. The most common control points for the

26 chronologies are radiocarbon dates (86.1%), calibrated by the latest calibration curves (IntCal20 and SHcal20 for  
27 the terrestrial radiocarbon dates in the northern and southern hemispheres; Marine20 for marine materials). The  
28 original ~~literature was~~publications were consulted when dealing with ~~obvious~~ outliers and inconsistencies. Several  
29 major challenges when setting up the chronologies included the waterline issue (18.8% of records), reservoir  
30 effect (4.9%), and sediment deposition discontinuity (4.4%). Finally, we numerically compare the LegacyAge 1.0  
31 chronologies to ~~the original ones~~those published in the original publications and show that the reliability of the  
32 chronologies of 95.4% of records could be improved according to our assessment. Our chronology framework  
33 and revised chronologies provide the opportunity to make use of the ages and age uncertainties in synthesis studies  
34 of, for example, pollen-based vegetation and climate change. The LegacyAge 1.0 dataset, including metadata,  
35 datings, harmonized chronologies, and R code used, are open-access and available at PANGAEA  
36 (<https://doi.pangaea.de/10.1594/PANGAEA.933132>; Li et al., ~~2021~~2021) and ~~GitHub~~Zenodo  
37 (<https://doi.org/10.5281/zenodo.5815192>; Li et al., 2022), respectively.

38

## 39 1 Introduction

40 Global and continental fossil pollen databases are used for a variety of paleoenvironmental studies, such as past  
41 climate and biome reconstructions, palaeo-model validation, and the assessment of human-environmental  
42 interactions (Gajewski, 2008; Gaillard et al., 2010; Cao et al., 2013; Mauri et al., 2015; Trondman et al., 2015;  
43 Marsicek et al., 2018; Herzschuh et al., 2019). Several fossil pollen databases have been successfully established  
44 (Gajewski, 2008; Fyfe et al., 2009), such as the European Pollen Database  
45 (<http://www.europeanpollendatabase.net>), the North American Pollen Database  
46 (<http://www.ncdc.noaa.gov/paleo/napd.html>), and the Latin American Pollen Database  
47 (<http://www.latinamericapollendb.com>); most of these data are now included in the Neotoma Paleoecology  
48 Database (<https://www.neotomadb.org/>; Williams et al., 2018). Chronologies and age control points are stored in  
49 these databases along with the pollen records.

50 However, to date, the metadata and dating results of these records are not available in a machine-readable  
51 format; furthermore, the chronologies have been established using a variety of methodologies, and the  
52 quantification of temporal uncertainty, particularly between records, remains a challenge ~~However, the inference~~  
53 ~~of temporal uncertainty remains a challenge because they are based on calibrated and uncalibrated <sup>14</sup>C ages and~~

54 ~~were established using various methodologies~~ (Blois et al., 2011; Giesecke et al., 2014; Flantua et al., 2016;  
55 Trachsel and Telford, 2017). Recently, the need for harmonized and consistent chronologies allowing for the  
56 accurate assessment of temporal uncertainty between records has ~~chronologies and an identical inference of~~  
57 ~~temporal uncertainties have~~ increased as studies are looking for spatiotemporal patterns using multi-record  
58 analyses (Jennerjahn et al., 2004; Blaauw et al., 2007; Giesecke et al., 2011; Flantua et al., 2016). Accordingly,  
59 some efforts ~~has~~ have been made to harmonize the chronologies for a subset of the records in these databases~~part~~  
60 ~~of the data stored in the databases~~ (Fyfe et al., 2009; Blois et al., 2011; Giesecke et al., 2011; Giesecke et al., 2014;  
61 Flantua et al., 2016; Brewer et al., 2017; Wang et al., 2019; ~~Mottl et al., 2021~~). However, a harmonized  
62 chronology framework is needed, not only to allow for the consistent inference of age and age uncertainties but  
63 also to apply to newly published records or one that can be adjusted to the specific requirement of a study.

64 Here we present the rationale and code, as well as the metadata and parameter settings for~~for~~ the chronology  
65 framework ~~named~~ LegacyAge 1.0, which contains harmonized chronologies for 2831 palynological records,  
66 synthesized from the Neotoma Paleocology Database (last access: April 2021, Neotoma hereafter) and the  
67 supplementary Asian datasets (Cao et al., 2013, 2020).~~as well as the metadata, and parameter settings of 2831~~  
68 ~~palynological records from the Neotoma Paleocology Database (last access: April 2021) and 324 additional Asian~~  
69 ~~records that were recently synthesized (Cao et al., 2013, 2020).~~ We also report on the major challenges ~~when of~~  
70 setting up the chronologies and assessing the their ~~quality of the LegacyAge 1.0 chronologies~~. Finally, the newly  
71 harmonized chronologies are numerically compared with the original ones. All data and R code used for this study  
72 are open-access and available at PANGAEA (<https://doi.pangaea.de/10.1594/PANGAEA.933132>; Li et al., 2021a)  
73 and Zenodo (<https://doi.org/10.5281/zenodo.5815192>; Li et al., 2022), respectively.

74

## 75 2 Methods

### 76 2.1 Data sources

77 We established harmonized chronologies for 3471 records in the ‘Global taxonomically harmonized late  
78 Quaternary pollen dataset’ (<https://doi.pangaea.de/10.1594/PANGAEA.929773>; Herzschuh et al., 2021). This  
79 compilation comprises 3147 records from Neotoma (last access: April 2021) and 324 Asian records from China  
80 and Siberia compiled by Cao et al. (2013, 2020) and from our own data (AWI). Records are ~~We established~~

81 ~~chronologies for the ‘Global taxonomically harmonized pollen data collection with revised chronologies’~~  
82 ~~(<https://doi.pangaea.de/10.1594/PANGAEA.929773>; Herzschuh et al., 2021), which comprises 3471 records~~  
83 ~~(3147 records from Neotoma (last access: April 2021) and 324 records from Asian datasets). Records were~~  
84 ~~obtained~~ from lake sediments (49.4%), peatlands (34.3%), and other archives (16.3%) (Fig. 1). ~~As the spatial~~  
85 ~~coverage of records in certain regions is poor, for example, in China and Siberia, records compiled by Cao et al.~~  
86 ~~(2013, 2020) and our own collection (AWI) were included.~~ The following chronology metadata were collected  
87 for each record: *Event*, *Data\_Source*, *Site\_ID*, *Dataset\_ID*, *Site\_name*, *Location* (*longitude*, *latitude*, *elevation*,  
88 *and continent*), *Archive\_Type*, *Site\_Description*, *Reference*, *Laboratory*, ~~*number of dating label*~~, *Dating\_Method*,  
89 *Material\_Dated*, *Date* (~~*uncalibrated and calibrated*~~ *age*, *error older*, *error younger*, *depth*, *thickness*), *Additional*  
90 *relevant comments from authors* (e.g., *reservoir effect*, *hiatus*, *outliers*, *and date rejected*); Furthermore,  
91 information on the original chronologies of each pollen record was also taken from the Neotoma and  
92 supplementary Asian datasets, including *Chronology name*, *Age type* (*calibrated or uncalibrated radiocarbon*  
93 *years BP*), *Pollen depth*, *Estimated age* (*age*, *age error*)). These metadata are available at  
94 <https://doi.pangaea.de/10.1594/PANGAEA.933132> (Supplement Table S1 and S4; Li et al., 2021). ~~*Original*~~  
95 ~~*chronologies* (*name*, *age type* (*calibrated or uncalibrated radiocarbon years BP*), *age model*, *estimated age* (*age*~~  
96 ~~*older*, *age*, *age younger*), *control points* (e.g., *core top*, *core bottom*, *and control point type*)). This dataset is~~  
97 ~~available at <https://doi.pangaea.de/10.1594/PANGAEA.933132> (Li et al., 2021).~~

98

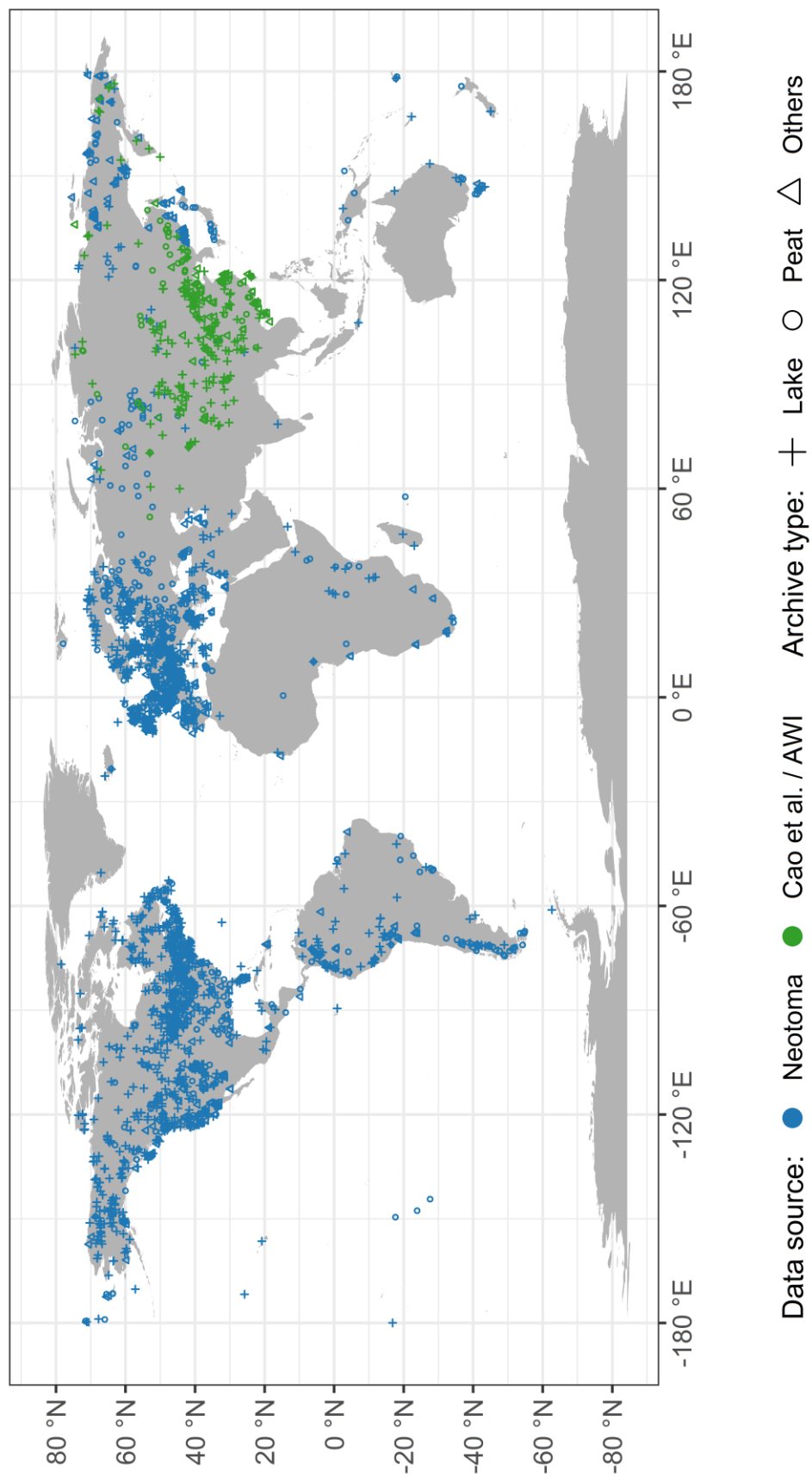


**Figure 1.** Map of records by source and archive type.

## 100 2.2 Chronological control points

### 101 2.2.1 Radiometric dates

102 *Radiocarbon dating*: most records ~~are~~ were dated using ~~by~~ radiocarbon-based methods ( $^{14}\text{C}$  dating, conventional  
 103 or accelerator mass spectrometry, Christie, 2018), ~~which is one of the most commonly used dating techniques as~~  
 104 ~~it covers the~~ covering the time range of ca. the last 50 kyr BP (before present, where ‘present’ is 1950 CE). ~~time~~  
 105 ~~range of most pollen records (ca. the last 50 ka BP (before present)).~~ However, the accuracy and precision of the  
 106 radiocarbon dates depend on the calibration curve, taphonomy, and dating materials (Blois et al., 2011; Heaton et  
 107 al., 2021). ~~However,  $^{14}\text{C}$  dates can appear to be too old or too young due to various effects such as the reservoir~~  
 108 ~~effect, contamination, and insufficient carbon, which have to be considered when setting up the chronologies~~  
 109 ~~(Roberts, 2013).~~

110 *Lead-210 dating*: the uppermost part of some lake records ~~have~~ has been dated using a radioactive isotope of lead  
 111 (lead-210), which has a half-life of ~~22.3~~ ca. 22 years and provides useful age control for the last ~~75400~~ 150 years.  
 112 However, the abundance of other radioactive isotopes (e.g., Caesium-137) affects the accuracy and precision of  
 113 the calibration curve for lead-210, resulting in temporal uncertainty (Appleby and Oldfield, 1978; Cuney, 2021).

114 *Luminescence dating*: archaeological materials, loess, and river sediments have often been dated via  
 115 luminescence, including thermoluminescence (TL) and optically stimulated luminescence (OSL), which cover  
 116 time scales. ~~These dating techniques cover time scales~~ from millennia to hundreds of thousands of years (Roberts,  
 117 2013; Cuney, 2021). Due to the systematic and random errors in the measurement process, the luminescence ages  
 118 have at least 4-5% uncertainty, which widens with increasing time (Wallinga and Cunningham, 2015).

### 119 2.2.2 Lithological dates

120 *Varve dating*: varve chronology, generated from counting varves, is considered a relatively accurate dating  
 121 method for the late Quaternary, particularly ~~for~~ the Holocene. Although sediment characteristics (e.g., thickness,  
 122 continuity, marking layer) may create uncertainty in varve-counted ages, these uncertainties are small relative to  
 123 those from radiometric methods (Ojala et al., 2012; Zolitschka et al., 2015; Ramisch et al., 2020). If a pollen  
 124 record has a varve chronology stored and assessed in the Varved Sediments Database (VARDA, [https://varve.gfz-](https://varve.gfz-potsdam.de/)  
 125 [potsdam.de/](https://varve.gfz-potsdam.de/)), we generally prefer to use it over chronologies based on other dating techniques.

126 **Tephrochronology:** tephra layers are used as isochrones to correlate and synchronize sequences at a regional or  
127 continental scale (Lowe, 2011). The uncertainties of tephrochronology are similar to those known in radiocarbon  
128 dating, such as methodological and dating errors (Flantua et al., 2016). Tephras documented in the Global  
129 Tephrochronological Database (Tephabase, <https://www.tephrabase.org/>) were included to improve the  
130 chronologies, ~~(in accordance with Giesecke et al., 2014),~~ such as the Mazama ash (7630±40 cal. yr BP; Brown  
131 and Hebda, 2003), Vedde ash (12121±57 cal. yr BP; Lane et al., 2012), and the Laacher See ash (12880±120  
132 cal. yr BP).

### 133 2.2.3 Biostratigraphical dates

134 Biostratigraphical dates have been widely relied on before <sup>14</sup>C dating became available and affordable (Bardossy  
135 and Fodor, 2013). We ignored most of the available biostratigraphical dates when we harmonized the chronologies  
136 because vegetation reaction to climate change is likely not sufficient synchron. Only a few well-known and widely  
137 applicable biostratigraphic boundaries (Rasmussen et al., 2014) were used in other dating techniques that could  
138 not sufficiently constrain the chronologies.~~Since the biostratigraphic schemes are updated by new records,~~  
139 ~~improved dating, and taxonomic revision (Flantua et al., 2016), most of them were rejected when we harmonized~~  
140 ~~the chronologies. However, a few well known and widely applicable biostratigraphic boundaries (Rasmussen et~~  
141 ~~al., 2014) were used if the chronologies could not be sufficiently constrained by other dating techniques,~~ for  
142 example, the Younger Dryas/Holocene (11500±250 cal. yr BP), Allerød/Younger Dryas (12650±250 cal. yr BP),  
143 and Oldest Dryas/Bølling (14650±250 cal. yr BP; Giesecke et al., 2014).

144

## 145 2.3 Establishing the chronologies

### 146 2.3.1 Method choice

147 We used the Bacon software (Blaauw and Christen, 2011) to establish continuous down-core chronologies from  
148 the age control points. Bacon fits a monotonic autoregressive (AR1) model to age control points using Bayesian  
149 methods to combine information from the control points with prior information on the statistical properties of  
150 accumulation histories for deposits, e.g., a prior distribution for the mean accumulation rate and how it varies  
151 (Blaauw and Christen, 2011). Several other approaches are available for age-depth modeling, including linear  
152 interpolation, smoothing splines, and other Bayesian methods, e.g., OxCal (Ramsey, 2008) and Bchron (Haslett

153 and Parnell, 2008). However Bacon has become one of the most frequently used and compares well with other  
154 methods (Trachsel and Telford, 2017, Blaauw et al., 2018). Establishing age-depth relationships is necessary  
155 because sediment cores typically have fewer chronological control points than samples and to account for dating  
156 uncertainty. A number of methods are available including linear interpolation, smoothing spline, OxCal, Behron,  
157 and Bacon (Bennett and Fuller, 2002; Blaauw, 2010; Blaauw and Heegaard, 2012; Flantua et al., 2016; Sánchez  
158 Goñi et al., 2017; Trachsel and Telford, 2017; Blaauw et al., 2018). Bacon is one of the most commonly used  
159 methods for age-depth modeling that ‘uses Bayesian statistics to reconstruct Bayesian accumulation histories for  
160 deposits, through combining radiocarbon and other dates with prior information’ (Blaauw and Christen, 2011).  
161 The collection of additional information, on the geological and hydrological setting as well as the environmental  
162 history (Giesecke et al., 2014), helps to constrain the chronologies, although it is time-consuming for large datasets.  
163 Through millions of Markov Chain Monte Carlo (MCMC) iterations, — Bacon provides the calibrated ages (mean,  
164 median, minimum, maximum) at each depth (e.g., every centimeter) with a 95% confidence intervals and an  
165 indication of how well the model fits the dates, although it needs much supervision and computing power. The  
166 prior distribution confidence interval guides the overall trend of the age-depth relationships, so the control points  
167 guide rather than strictly constrain the age-depth relationships (Giesecke et al., 2014). Bacon version 2.3.3 and  
168 later (Blaauw and Christen, 2011) can also handle sudden shifts in the accumulation rate when given the  
169 hiatus/boundary depth and resetting the memory to 0 when crossing the hiatus. Therefore, all age-depth  
170 relationships in our dataset will be constructed using the latest Bacon version 2.5.3 (Blaauw and Christen, 2011;  
171 Blaauw et al., 2018) in R (R Core Team, 2021).

### 172 **2.3.2 Core tops and basal ages**

173 Wherever possible, the record-related publications were read to decide whether the core top was modern at the  
174 time of sampling. For modern core-tops, if the core was collected from sites where sediment was still accumulating,  
175 the sediment surface could be assigned to the year of sampling, adding one significant time control for the  
176 chronologies. If the sampling date was unavailable, an alternative surface age from the original chronology in  
177 Neotoma was added at the core top. An estimated artificial core-top age (-50 + -30 cal yr BP) was used if none of  
178 the above ages were available (Supplement Table S2, S3). We inferred the surface age from the calibrated age-  
179 depth model for core-tops judged not to be modern. For core tops judged not to be modern, we inferred the surface  
180 age from the calibrated age-depth model. For basal ages, when the calibrated age-depth model for the lowermost



181 profile has considerable extrapolation and was not sufficiently constrained by the control points, we also accepted  
 182 the prior information of core basal age from the record-related publications or Neotoma. ~~Moreover, the highest~~  
 183 ~~(lowest) depth of the model was defined by the first (last) dating or pollen sample.~~

### 184 2.3.3 Calibration curves

185 To transform the measured  $^{14}\text{C}$  ages to calendar ages, the latest calibration curves, approved by the radiocarbon  
 186 community (Hajdas, 2014), were used in Bacon routine~~were used; (Hajdas, 2014);~~ IntCal20 (Reimer et al., 2020;  
 187 Heaton et al., 2021) and SHcal20 (Hogg et al., 2020) to calibrate the terrestrial radiocarbon dates in the northern  
 188 and southern hemispheres, respectively; and Marine20 (Heaton et al., 2020) for the 38 marine records included in  
 189 our dataset ~~although it does not distinguish between the northern and southern hemisphere~~ (Sánchez Goñi et al.,  
 190 2017). The numerical probability distributions of calendar age from calibrated radiocarbon dates were summarised  
 191 to a mean and standard deviation for use in Bacon. Absolute dates (e.g., lead-210, OSL, tephra), already presented  
 192 on the calendar scale, were not calibrated (Blaauw and Christen, 2011). Modern/post-bomb  $^{14}\text{C}$  dates (negative  
 193  $^{14}\text{C}$  ages) were calibrated using appropriate post-bomb calibration curves (post-bomb=1 for  $>40^\circ\text{N}$ ; 2 for  $0^\circ$ - $40^\circ\text{N}$ ;  
 194 4 for southern hemisphere; Hua et al., 2013).

### 195 2.3.4 Parameter settings for the initial Bacon run

196 After consultation of the relevant literature publication (Blaauw and Christen, 2011; Goring et al., 2012; Cao et  
 197 al., 2013; Fiałkiewicz-koziół et al., 2014; Blaauw et al., 2018) and assessments of several runs with a test set of  
 198 records, we set the following Bacon parameters (Supplement Table S3):-

- 199 (1) The prior for the accumulation rate consists of a gamma distribution with two parameters, **mean accumulation**  
 200 **rate** (~~acc.rate~~acc.mean; default 20 yr cm<sup>-1</sup>) and **accumulation shape** (acc.shape; default 1.5). For the  
 201 acc.shape, we accepted its default value ~~of 1.5~~ as higher values resulted in a more peaked shape of the gamma  
 202 distribution. A first approximation of the acc.mean was calculated as the average accumulation rate between  
 203 the first and the last date of each record, combined with the prior information of dates, which is more  
 204 reasonable than using a constant value (~~default acc.mean=20 yr/cm~~).
- 205 (2) Bacon divides a core into many vertical sections of equal thickness (thick; default 5 cm), which significantly  
 206 affects the flexibility of the age-depth model, and through millions of Markov Chain Monte Carlo iterations  
 207 estimates the accumulation rate for each section. The section thickness (default thick=5) significantly affects

~~the flexibility of the age-depth model.~~ Blaauw and Christen (2011) indicated that models with few sections tend to show more abrupt changes in accumulation rate, while models with many sections usually appear smoother but are computationally more intense. We run Bacon for six section thicknesses (2.5 cm, 5 cm, 10 cm, 30 sections, 60 sections, and 120 sections), optimal values after numerous tests, with and without core-top age resulting in 12 initial chronologies for each record. We tested six thicknesses (2.5 cm, 5 cm, 10 cm, 30 sections, 60 sections, and 120 sections) with and without an artificial surface age, thereby generating 12 age models for each core.

(3) The prior for the memory, that is, the dependence of accumulation rate between neighboring depths, is a beta distribution defined by two parameters: **memory strength** (mem.strength; default 10) and **mean memory** (mem.mean; default 0.5). For the mem.strength, we used a value of 20 as suggested by Goring et al. (2012), which allows a large range of posterior memory values. We set different mem.mean values (0.3 for lake and 0.7 for peatland) to accommodate differences in accumulation conditions between lakes and peatland, where the higher memory for peatlands implies a more constant accumulation history (Blaauw and Christen, 2011; Goring et al., 2012; Cao et al., 2013; Cao et al., 2020).

(4) The **minimum (maximum) depth** (d.min and d.max, respectively) of the age-depth model was defined by the uppermost (lowermost) dating or pollen sample depth (Supplement Table S4). The parameter ‘d.by’ (default 1 cm) defines the **depth intervals** at which ages are calculated, and we accepted its default value.

In addition to the major parameters mentioned above, we also adjusted several ~~specific~~ additional parameters for ~~some individual~~ records according to prior information collected from record-related publications or Neotoma (Supplement Table S2, S3~~this table is available in PANGAEA~~).

(1) ~~**RFreshwater reservoir effects:** the uptake of old carbon by aquatic plants, mosses, or shells either originating from, e.g., limestone in the catchment (‘hard-water effect’) or slow <sup>14</sup>C exchange between the atmosphere and ocean interior, can result in too old radiocarbon dates (Philippsen, 2013; Philippsen and Heinemeier, 2013; Giesecke et al., 2014; Heaton et al., 2020). the uptake of old carbon by aquatic plants, the ‘hard water effect’ or slow CO<sub>2</sub> exchange between the atmosphere and water, can result in too old radiocarbon dates (Philippsen, 2013; Philippsen and Heinemeier, 2013).~~ In addition to the reservoir ages reported by the original authors, we also identified some additional records for which there is likely a reservoir effect through modern correction and linear extrapolation (Wang et al., 2017). In addition to the reservoir ages reported by the original authors,

236 ~~we also identified some additional records, where the authors may have ignored them via modern correction~~  
237 ~~and linear extrapolation (Wang et al., 2017).~~ We then subtracted the reservoir age as a constant from all  $^{14}\text{C}$   
238 ~~dates of an affected record, excluding those derived from terrestrial macrofossils.~~ We then subtracted the  
239 ~~reservoir age from all  $^{14}\text{C}$  dates of an affected record as a constant.~~ We may have underestimated the number  
240 of such records due to the difficulty of estimating the reservoir age where the sediment surface was eroded or  
241 used for agricultural purposes.

242 (2) **Waterline issues:** stratigraphic records do not always start at a depth of 0 cm, for example, if the uppermost  
243 part of the core is lost, if the record is only a part of a longer sequence, or if the depths are measured from the  
244 water surface instead of the sediment surface, leading to the so-called waterline issue. Accordingly, we  
245 adjusted the uppermost depth of the chronology based on ~~prior~~ information collected from the original  
246 publications and Neotoma.

247 (3) **Hiatuses:** ~~where sediment deposition was not continuous, it is possible to set a “hiatus” at which Bacon resets~~  
248 ~~the memory to 0, causing a break in the autocorrelation in the accumulation rate for depths before and after~~  
249 ~~the hiatus and additionally models an instantaneous jump in age at that depth (Blaauw and Christen,~~  
250 ~~2011).~~ ~~where the sediment deposition was not continuous, Bacon resets the memory to 0, causing a break in~~  
251 ~~auto-correlated in the accumulation rate for depths before and after the hiatus (Blaauw and Christen, 2011).~~

252 (4) **Dates rejected/added:** Neotoma usually reports all  $^{14}\text{C}$  dates from cores, even when deemed inaccurate. We  
253 assessed prior information on dates and then excluded the  $^{14}\text{C}$  dates of samples with contaminated or reworked  
254 sediments from age-depth model from age-depth models. ~~We assessed and, if appropriate, a priori rejected the~~  
255  ~~$^{14}\text{C}$  dates of samples with contaminated or insufficient carbon, or reworked sediments,~~ in most cases following  
256 the suggestions in the original publications. For example, we excluded the date at 164 cm, accepted by the  
257 author (Gajewski et al., 2000), from the Muskoka Lake record (ID 1783), as it does not agree with the other  
258 three dates from the same core and where lithology had changed significantly at that depth. We down-weighted  
259 the impact of outliers on the overall trend of the age-depth relationships and risked that age uncertainties were  
260 too optimistic. We also documented all lithological dates (e.g., varves and tephra) and biostratigraphical dates  
261 collected from the original publications and ~~from~~ Neotoma to supplement the chronology metadata.

### 262 2.3.5 Assessment of initial age-depth models and final parameter selection

263 To objectively evaluate the 12 initial age-depth models for each record, we initially tested a least-squares method  
264 between the age model and ages of dated depths and calculated the mean uncertainty for each model. However,  
265 the least-squares method is susceptible to outliers (Birks et al., 2012), and models with least-squares may risk  
266 more abrupt changes in accumulation rate due to over-fitting dates. Instead of a numerical comparison, we finally  
267 implemented a visual comparison based on the Bacon output graphs, which show the Markov Chain Monte Carlo  
268 iterations, the prior and posterior distributions for the accumulation rate and memory, and how well the model fits  
269 the date (Blaauw and Christen, 2011).

270 Preference was given to models that fitted the dates well, had small mean uncertainties (Supplement Table S5),  
271 and good runs of Markov Chain Monte Carlo iterations (i.e., a stationary distribution with little structure among  
272 neighboring iterations as indicated by the traceplot of the joint likelihood) when visual choosing the ‘best’ model  
273 for each record (Blaauw and Christen, 2011; Blaauw et al., 2018). For each record, 12 age models were visually  
274 assessed. Preference was given to models that fitted the dates well and with small uncertainties when choosing  
275 the ‘best’ model for each record (Blaauw and Christen, 2011; Blaauw et al., 2018). If necessary, we also-adjusted  
276 the parameter settings such as the section thickness and mean- accumulation rate to ~~make a~~ better fit with the  
277 dates that ~~was were~~ consistent with prior information. For the final parameter settings used for each record, please  
278 see <https://doi.pangaea.de/10.1594/PANGAEA.933132> (Supplement Table S3; Li et al., 2021).

279

### 280 2.4 Evaluation of the newly generated age-depth models

281 For the temporal uncertainty of the age-depth models, we take used the 95% confidence intervals for age estimated  
282 by the Bacon model for each centimeter (Supplement Table S5). These values are approximately twice the  
283 standard error of the estimated age at a given depth. We plotted our newly generated ‘best’ calibrated chronologies  
284 with 95% confidence intervals together with the original ones taken from the Neotoma and Cao et al. (2013, 2020)  
285 datasets (Supplement Table S4) to compare and evaluate the performance of the new models visually to make  
286 ~~comparisons and evaluate the performance of the new models.~~ The criteria for the preferred models are that the  
287 model fitted the dates well, had small uncertainties, combined dates with prior information (e.g., geological and  
288 hydrological setting, environmental history), and calibrated with the latest calibration curves.

289

## 290 3 Results

### 291 3.1 Overview of major challenges when establishing the chronologies

292 Age-depth models were initially established for all 3471 records in the harmonized pollen data collection  
293 (Herzschuh et al., 2021). We discarded 640 records with fewer than two reliable dates (i.e., no reliable date  
294 or only one reliable date), evaluated based on prior information from original literature, leaving chronologies for  
295 2831 records. ~~Age-depth models were initially established for all 3471 records. We discarded 640 records with~~  
296 ~~fewer than 2 reliable dates and leaving chronologies for 2831 records.~~ We faced several major challenges when  
297 establishing the chronologies. After assessments and consultation of prior information from original publications  
298 (Supplement Table S2, S3), we identified 139 records (4.9%) with reservoir effects, 533 records (18.8%) with  
299 waterline issues, 125 records (4.4%) with hiatuses, 924 records (32.6%) with rejected or added dates, and 743  
300 records (26.2%) that contained several of the above problems: all these challenges have been handled (Fig. 2).  
301 After assessing initial age-depth models, accumulation rates were adjusted for 367 records (13.0%), and different  
302 section thicknesses were applied to 411 records (14.5%).

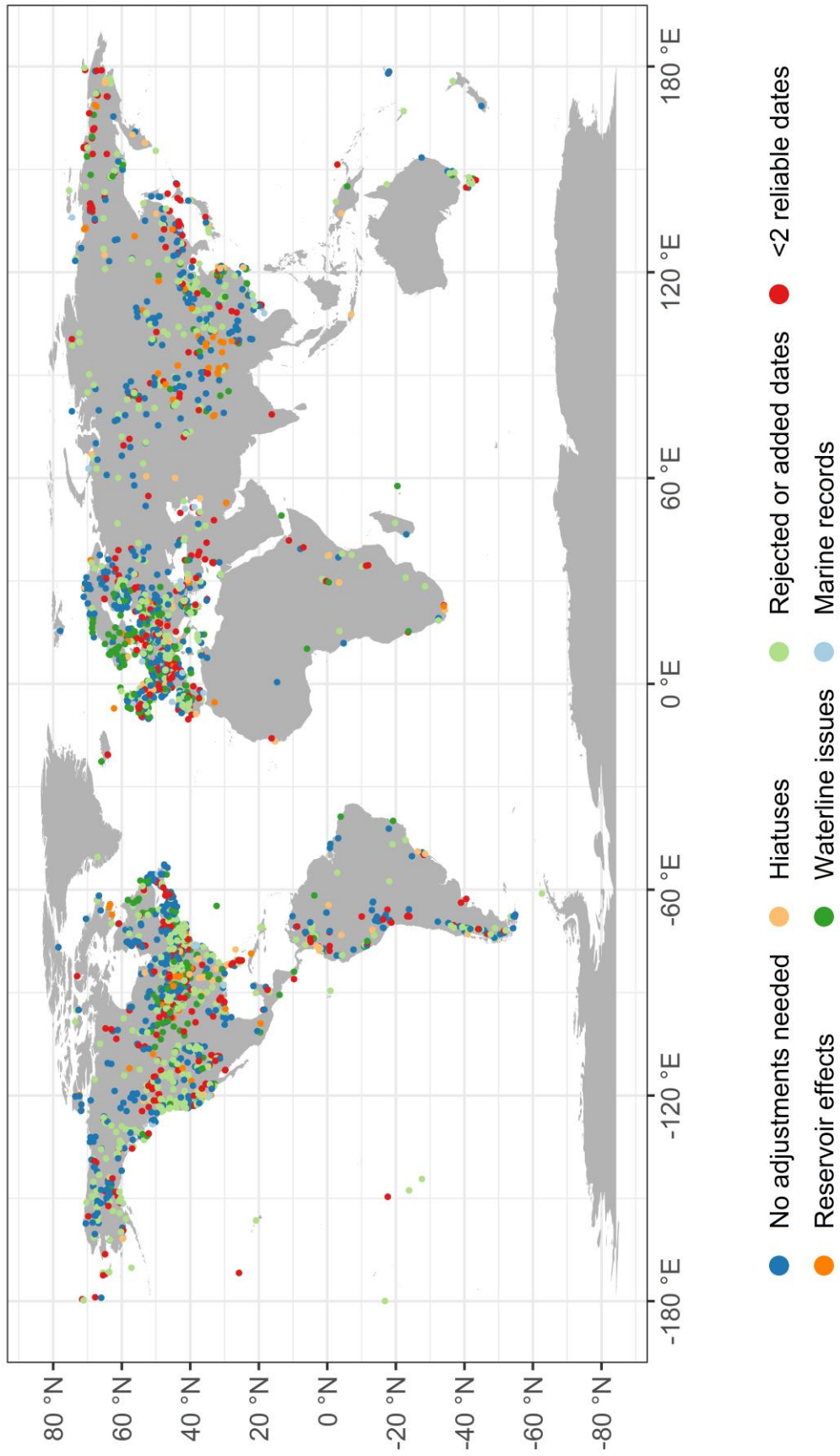


**Figure 2.** The distribution of records that faced various major challenges when establishing their chronologies.

## 304 3.2 LegacyAge 1.0 quality

### 305 3.2.1 Dates used for final chronologies

306 A total of 19,990 control points (out of 21,199 dates available) were used to generate the chronologies for the  
307 2831 records [\(Supplement Table S1\)](#). Among them, the most common chronological control points are  
308 radiocarbon dates (86.1%), followed by lithological and biostratigraphical dates (8.5%) collected from  
309 publications or Neotoma, and lead-210 (5.0%); other dating techniques make up 0.4% of the control points. The  
310 median number of dates per chronology is 5, with 23.3% of the chronologies having 2 or 3 dates, 53.3% having  
311 4-8 dates, and 23.4% having at least 9 dates (Fig. 3).

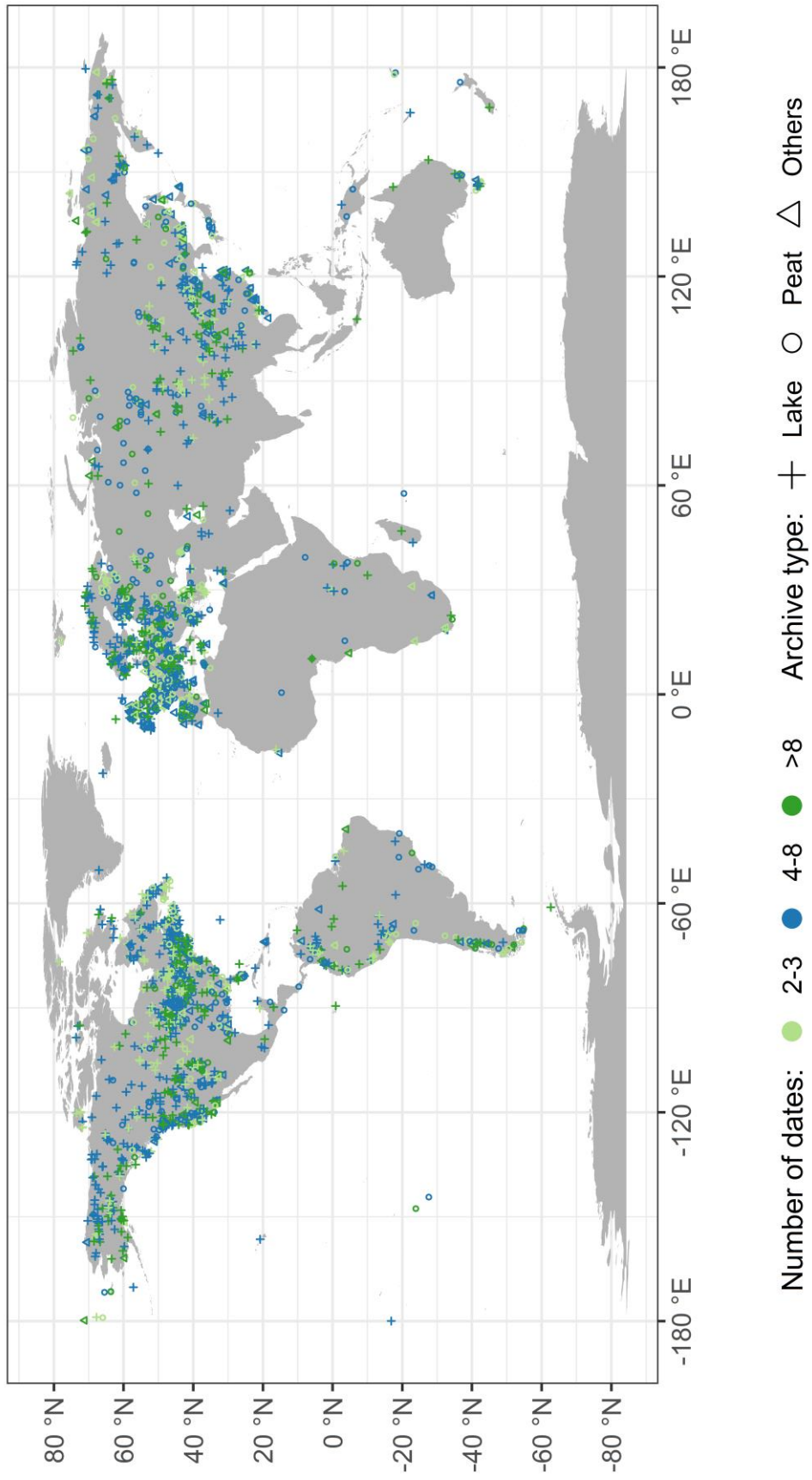
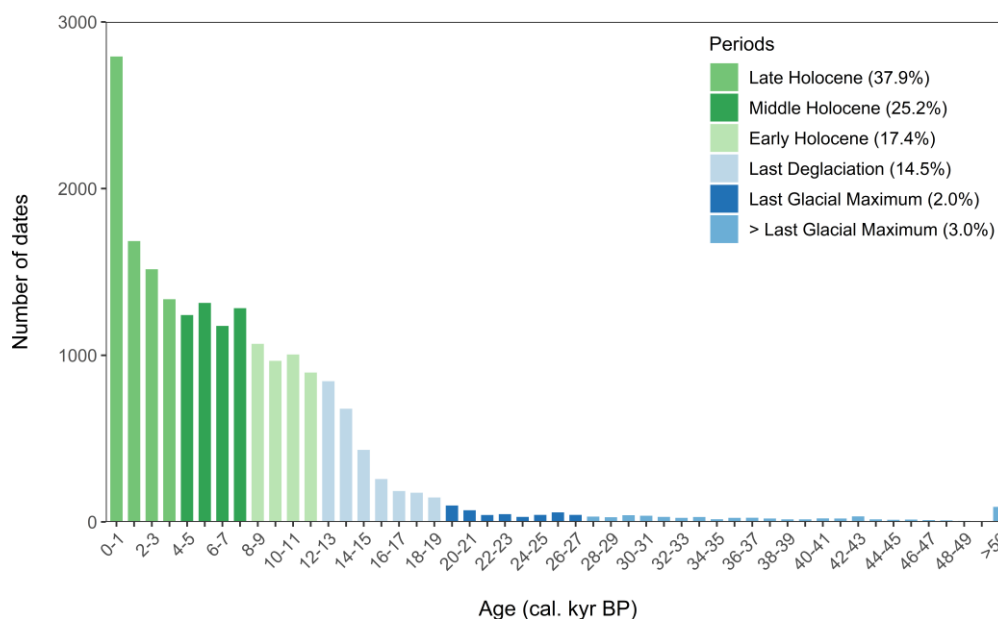


**Figure 3.** Map of the number of dates and archive types for each record.



313 Currently, 80.5% of chronological control points in the LegacyAge 1.0 fall within the Holocene (37.9%, 25.82%,  
 314 and 16.817.4% within the late (ca. 0-4.2 cal. ~~kyr~~ BP), middle (ca. 4.2-8.38.2 cal. ~~kyr~~ BP), and early Holocene  
 315 (ca. 8.38.2-11.7 cal. ~~kyr~~ BP), respectively), 14.5% within the Last Deglaciation (ca. 19.0-11.711.7-19.0 cal.  
 316 ~~kyr~~ BP; Clark et al., 2012), 2.0% within the Last Glacial Maximum (LGM; ca. 26.5-19.019.0-26.5 cal. ~~kyr~~  
 317 BP; Clark et al., 2009), and only 3.0% earlier than the LGM (Fig. 4).



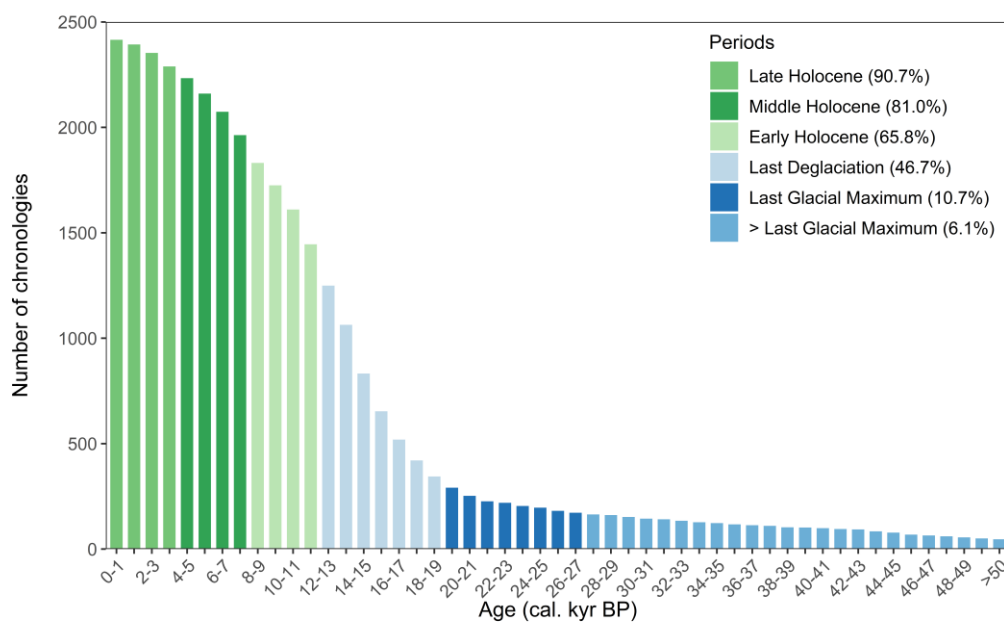
318

319 **Figure 4.** Histogram showing the number of available dates in distinct time slices.

### 320 3.2.2 Spatial and temporal coverage

321 Of the 2831 chronologies finally established, 1032 records are from North America, 1075 records from Europe,  
 322 488 records from Asia, 150 records from South America, 54 records from Africa, and 32 records from the Indo-  
 323 Pacific (Fig. 3). Most records (2659 records, 93.9%) are in the northern hemisphere, where the main vegetation  
 324 and climate zones are covered.

325 As shown in Fig. 5, 94.8% of chronologies cover part of the last 30 ~~kyr~~, while Marine Isotope Stage 3 (MIS-  
 326 3) is relatively poorly covered. Specifically, 98.0% of chronologies cover part of the Holocene (90.7%, 81.0%,  
 327 and 65.8% cover part of the late, middle, and early Holocene, respectively), 46.7% cover part of the Last  
 328 Deglaciation, 10.7% cover part of the Last Glacial Maximum, and only 6.1% earlier than LGM.



329

330 **Figure 5.** Histogram showing the number of available chronologies in distinct time slices.

### 331 3.2.3 Temporal uncertainty

332 Boxplots of age uncertainties for all chronologies in distinct time slices (Fig. 6), excluding outliers (ca. 4.25.1%),

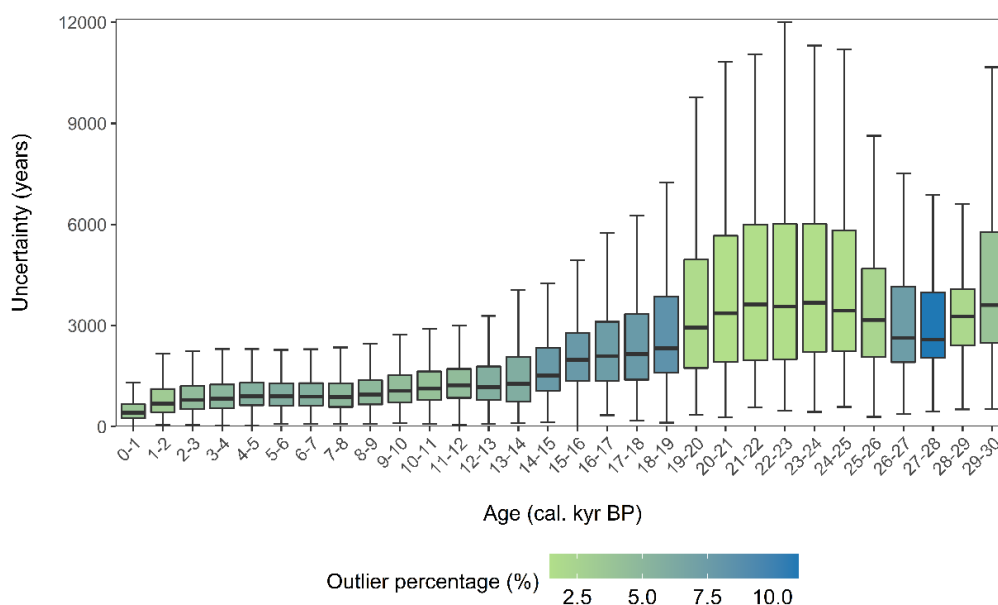
333 illustrate that age uncertainty tends to increase with age and ~~are~~ are mainly related to the uncertainty and precision

334 of the chronological control points, calibration curves, and age models~~uncertainties of the chronological control~~

335 ~~points and the uncertainty of the calibration curves~~ (Fig. 6 Blois et al., 2011). The boxplots show wide boxes,

336 i.e., a more extensive data range, for the LGM period, characterized by fewer outliers, mostly from chronologies

337 with sparse age control points and significant dating errors, than the periods with small box sizes.



338

339

**Figure 6.** Boxplots of age uncertainties and outlier percentages in distinct time slices.

340

### 3.3 Comparison of the LegacyAge 1.0 vs. original age-depth models

341

For 906 records out of the 2831 records included in the LegacyAge 1.0, no calibrated chronologies were originally available from the Neotoma and Cao et al. (2013, 2020) datasets for comparison. Of the remaining 1925 records, the new LegacyAge 1.0 chronologies were selected instead of the original ones in 95.4% of cases, based on the aforementioned criteria. However, some records still chose the original chronology, mainly ~~Where original chronologies outperformed LegacyAge 1.0, it is mainly~~ because they are varve chronologies, had incomplete metadata (e.g., missing sample depths), or ~~they~~ included some non-<sup>14</sup>C dates that our model could not accommodate (Supplement Table S6).

348

In most cases, the newly established chronologies were rather similar to the original ones. For 1012 records (52.6% of 1925 records), the original chronologies were within the 95% confidence intervals of the LegacyAge 1.0 chronologies, while the other 913 records (47.4%) were partially or completely outside the 95% confidence intervals.

352

Selected typical examples of the comparative results between the accepted LegacyAge 1.0 chronologies, alternative newly generated but rejected chronologies, and the original chronologies ~~Selected typical examples of the comparison results between the newly generated and original chronologies~~ are illustrated in Fig. 7. For the *EL Tiro-Pass* record (ID 47502, Fig. 7a), both the original and LegacyAge 1.0 newly generated chronologies were

355

356 established by Bacon and are acceptable. However, ~~our the LegacyAge 1.0 newly generated~~ chronology has the  
357 advantage that it makes use of the latest radiocarbon calibration curve (IntCal20; Reimer et al., 2020), and the  
358 estimated surface age is more realistic as sediments are still accumulating (Niemann and Behling, 2008). For the  
359 *Fargher Pond* record (ID 15344, Fig. 7b), ~~our the LegacyAge 1.0 newly generated~~ chronology includes more varve  
360 ages from the Varved Sediments Database. These provide a better constraint for the lowermost profile than the  
361 original model had (Grigg and Whitlock, 2002). For the *Oltush Lake* record (ID 4320, Fig. 7c), the  $^{14}\text{C}$  age of  
362 modern sediment in this lake is 350 yr BP and thus, the assumption of a reservoir effect of 350 years resulted in  
363 slightly younger ages than originally given (Davydova and Servant-Vildary, 1996). Some alternative rejected  
364 chronologies performed poorly due to the inability of high-resolution Bacon models to accommodate  
365 accumulation rate changes (Fig. 7b and Fig. 7c). Finally, for the *Soppensee* record (ID 44723, Fig. 7d), most of the  
366  $^{14}\text{C}$  dates (> 540 cm) come from samples with insufficient carbon to achieve accurate dating (Hajdas and  
367 Michczyński, 2010), and thus the original chronology, generated from counting varves, outperformed our newly  
368 generated chronologies. Finally, for the *Soppensee* record (ID 44723, Fig. 7d), most of the  $^{14}\text{C}$  dates (> 540 cm)  
369 have insufficient carbon and thus the original chronology, generated from counting varves, outperformed our  
370 newly generated chronology.

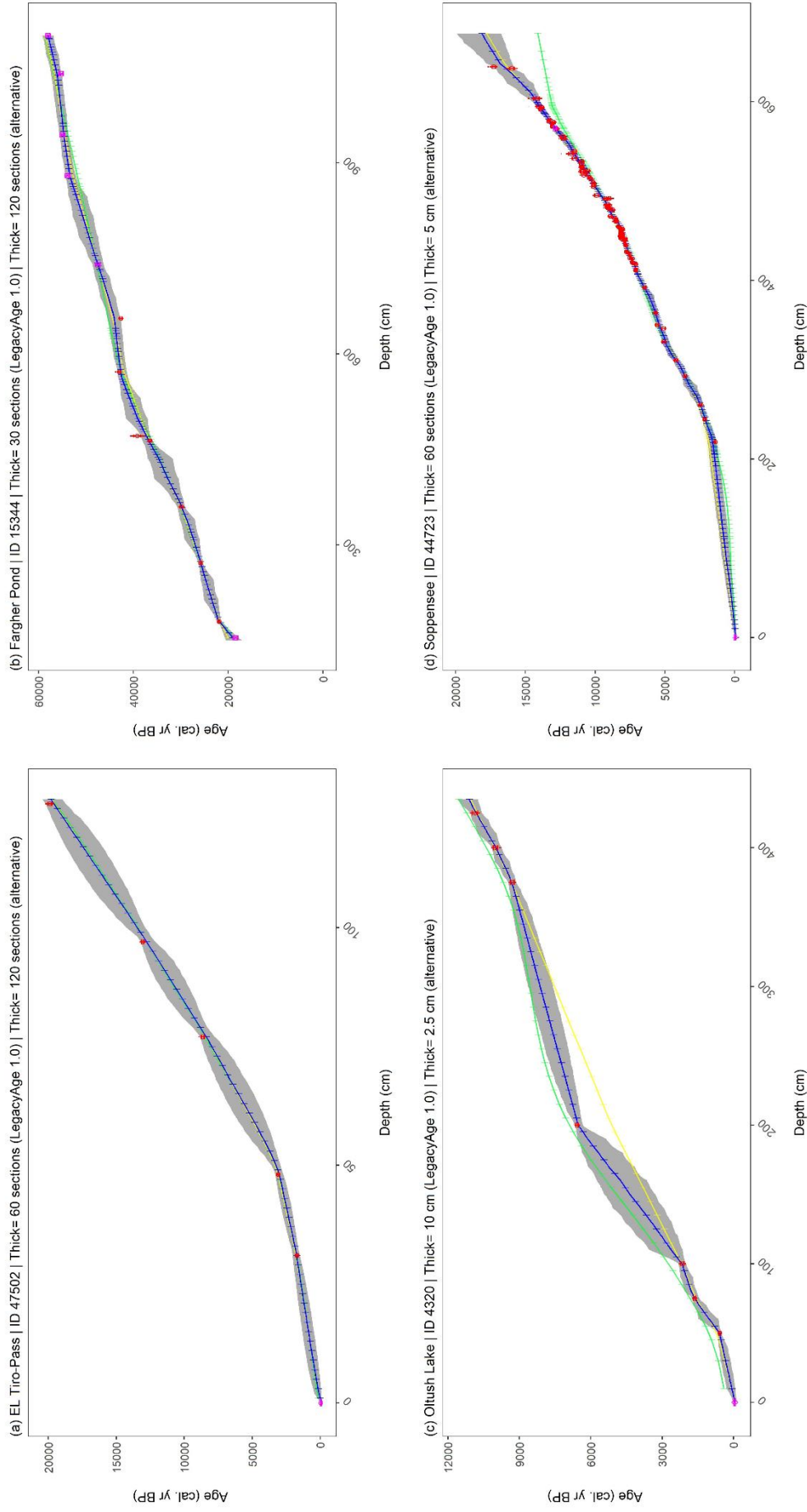


**Figure 7.** Comparison of LegacyAge 1.0 chronologies with the original ones. Green line: original chronology. Blue line: LegacyAge 1.0 chronology. Green line: original chronology. Blue line: LegacyAge 1.0 chronology. Yellow line: alternative newly generated but rejected chronology. Red: date in chronology metadata. Pink: date from prior information. Grey shading: age

#### 372 **4 Code and data availability**

373 All data and R code used for this study are available at PANGAEA  
374 (<https://doi.pangaea.de/10.1594/PANGAEA.933132>; Li et al., 2021) and Github  
375 (<https://github.com/LongtermEcology/ProxyAge-1.0>), respectively. Seven supplementary datasets (Table S1-S7,  
376 in comma-separated values format) and one readme text about the LegacyAge 1.0 are accessible in the navigation  
377 bar ‘Further details’ of the PANGAEA page (<https://doi.pangaea.de/10.1594/PANGAEA.933132>; Li et al., 2021).  
378 We provided the chronological control points metadata (Table S1), prior information of dates from publication  
379 (Table S2), Bacon parameter settings (Table S3), original chronology metadata from the Neotoma and Cao et al.  
380 (2013, 2020) (Table S4), LegacyAge 1.0 chronology (Table S5), description of the comparison of original  
381 chronology and LegacyAge 1.0 (Table S6), and record references (Table S7) respectively. All datasets are in long  
382 data format.

383 The R-code for calculation and comparison of chronologies with embedded manual, metadata for code runs,  
384 Bacon output graphs of each record, graphs comparison of original chronologies and LegacyAge 1.0, and a short  
385 shared-screen video of the R-code to show the usage on two example records are accessible on Zenodo  
386 (<https://doi.org/10.5281/zenodo.5815192>; Li et al., 2022).

387

#### 388 **5 How to use the LegacyAge 1.0 dataset and code**

389 LegacyAge 1.0 provides the calibrated ages (mean, median, minimum, maximum) and uncertainties at each  
390 centimeter for each record with a 95% confidence interval (Supplement Table S5). All users can apply some  
391 interpolation algorithms in the chronologies, subsetted from the LegacyAge 1.0 dataset or outputted by our code,  
392 to assign ages for proxy depths of records.

393 As for the R-code, users only need to set the working directory where the Bacon results will be stored and input  
394 the record ID of interest to run it successfully. The manual and shared-screen video on R-code usage could provide  
395 helpful guidance for users, with or without some R-experience.

396

## 397 **5-6 Conclusion**

398 This paper presents the framework as well as metadata, machine-readable datings, R pipeline, chronologies, and  
399 age uncertainties of 2831 pollen ~~palynological~~ records synthesized from the Neotoma Paleocology Database (last  
400 access: April 2021) and 324 additional Asian records (Cao et al., 2013, 2020). Chronologies and uncertainties can  
401 be used ~~from for~~ synthesis works; metadata, datings, and pipelines can be used to reestablish the chronologies for  
402 customized purposes, and the framework can be used to establish chronologies for newly updated records.

403

404 **Author contributions.** UH and CL designed the chronology dataset. CL and TB compiled the metadata and prior  
405 information of the chronologies. AP and TB wrote the R scripts and ran the analyses under the supervision of UH  
406 and CL. AMD contributed an initial R script for creating age-depth models with Bacon. CL wrote the first draft  
407 of the manuscript under the supervision of UH. All authors discussed the results and contributed to the final  
408 manuscript.

409 **Competing interests.** The authors declare that they have no conflict of interest.

410 **Acknowledgements.** The majority of data were obtained from the Neotoma Paleocology Database  
411 (<http://www.neotomadb.org>). The work of data contributors, data stewards, and the Neotoma community is  
412 gratefully acknowledged. We would like to express our gratitude to all the palynologists and geologists who, either  
413 directly or indirectly, contributed pollen data and chronologies to the dataset. We thank Andrej Andreev, Mareike  
414 Wieczorek, and Birgit Heim from AWI for providing information on pollen records and data uploads. We also  
415 thank Cathy Jenks for language editing on a previous version of the paper. This study was undertaken as part of  
416 LandCover6k, a working group of Past Global Changes (PAGES), which in turn received support from the US  
417 National Science Foundation, the Swiss National Science Foundation, the Swiss Academy of Sciences, and the  
418 Chinese Academy of Sciences.

419 **Financial support.** This research has been supported by the European Research Council (ERC Glacial Legacy  
420 772852 to UH), the PalMod Initiative (01LP1510C to UH), and the China Scholarship Council (201908130165  
421 to CL).

422

423 **References**

424 Appleby, P. G. and Oldfield, F.: The calculation of lead-210 dates assuming a constant rate of supply of  
425 unsupported <sup>210</sup>Pb to the sediment, *Catena*, 5, 1–8, [https://doi.org/10.1016/S0341-8162\(78\)80002-2](https://doi.org/10.1016/S0341-8162(78)80002-2), 1978.

426 Bardossy, G. and Fodor, J.: Evaluation of uncertainties and risks in geology: new mathematical approaches for  
427 their handling, Springer Science & Business Media, Berlin, Germany, 230 pp., 2013.

428 ~~Birks, H. J. B., Lotter, A. F., Juggins, S. and Smol, J. P. eds.: Tracking environmental change using lake sediments:  
429 data handling and numerical techniques (Vol. 5), Springer Science & Business Media, Berlin, Germany, 751  
430 pp., 2012.~~

431 ~~Bennett, K. D. and Fuller, J. L.: Determining the age of the mid-Holocene *Tsuga canadensis* (hemlock) decline,  
432 eastern North America, *The Holocene*, 12, 421–429, <https://doi.org/10.1191/0959683602h1556rp>, 2002.~~

433 Blaauw, M. and Christen, J. A.: Flexible paleoclimate age-depth models using an autoregressive gamma process,  
434 *Bayesian Anal.*, 6, 457–474, <https://doi.org/10.1214/11-BA618>, 2011.

435 ~~Blaauw, M. and Heegaard, E.: Estimation of age-depth relationships, in: Tracking Environmental Change Using  
436 Lake Sediments, Volume 5: Data Handling and Numerical Techniques, edited by: Birks, H. J. B., Lotter, A. F.,  
437 Juggins, S., and Smol, J. P., Springer, Dordrecht, Netherlands, 379–413, [https://doi.org/10.1007/978-94-007-  
2745-8\\_12](https://doi.org/10.1007/978-94-007-<br/>438 2745-8_12), 2012.~~

439 Blaauw, M., Christen, J. A., Bennett, K. D., and Reimer, P. J.: Double the dates and go for Bayes — Impacts of  
440 model choice, dating density and quality on chronologies, *Quat. Sci. Rev.*, 188, 58–66,  
441 <https://doi.org/10.1016/j.quascirev.2018.03.032>, 2018.

442 Blaauw, M., Christen, J. A., Mauquoy, D., van der Plicht, J., and Bennett, K. D.: Testing the timing of radiocarbon-  
443 dated events between proxy archives, *The Holocene*, 17, 283–288, <https://doi.org/10.1177/0959683607075857>,  
444 2007.

445 ~~Blaauw, M.: Methods and code for ‘classical’ age-modelling of radiocarbon sequences, *Quat. Geochronol.*, 5,  
446 512–518, <https://doi.org/10.1016/j.quageo.2010.01.002>, 2010.~~



- 447 Blois, J. L., Williams, J. W. J., Grimm, E. C., Jackson, S. T., and Graham, R. W.: A methodological framework  
448 for assessing and reducing temporal uncertainty in paleovegetation mapping from late-Quaternary pollen  
449 records, *Quat. Sci. Rev.*, 30, 1926–1939, <https://doi.org/10.1016/j.quascirev.2011.04.017>, 2011.
- 450 Brewer, S., Giesecke, T., Davis, B. A. S., Finsinger, W., Wolters, S., Binney, H., de Beaulieu, J. L., Fyfe, R., Gil-  
451 Romera, G., Köhl, N., Kuneš, P., Leydet, M., and Bradshaw, R. H.: Late-glacial and Holocene European pollen  
452 data, *J. Maps*, 13, 921–928, <https://doi.org/10.1080/17445647.2016.1197613>, 2017.
- 453 Brown, K. J. and Hebda, R. J.: Coastal rainforest connections disclosed through a Late Quaternary vegetation,  
454 climate, and fire history investigation from the Mountain Hemlock Zone on southern Vancouver Island, British  
455 Columbia, Canada, *Rev. Palaeobot. Palynol.*, 123, 247–269, [https://doi.org/10.1016/S0034-6667\(02\)00195-1](https://doi.org/10.1016/S0034-6667(02)00195-1),  
456 2003.
- 457 Cao, X., Ni, J., Herzschuh, U., Wang, Y., and Zhao, Y.: A late Quaternary pollen dataset from eastern continental  
458 Asia for vegetation and climate reconstructions: Set up and evaluation, *Rev. Palaeobot. Palynol.*, 194, 21–37,  
459 <https://doi.org/10.1016/j.revpalbo.2013.02.003>, 2013.
- 460 Cao, X., Tian, F., Andreev, A., Anderson, P. M., Lozhkin, A. V., Bezrukova, E., Ni, J., Rudaya, N., Stobbe, A.,  
461 Wiczorek, M., and Herzschuh, U.: A taxonomically harmonized and temporally standardized fossil pollen  
462 dataset from Siberia covering the last 40 kyr, *Earth Syst. Sci. Data*, 12, 119–135, [https://doi.org/10.5194/essd-](https://doi.org/10.5194/essd-12-119-2020)  
463 [12-119-2020](https://doi.org/10.5194/essd-12-119-2020), 2020.
- 464 [Christie, M.: Radiocarbon dating, WikiJournal of Science, 1, 1-17,](https://search.informit.org/doi/10.3316/informit.802309866976635)  
465 <https://search.informit.org/doi/10.3316/informit.802309866976635>, 2018.
- 466 Clark, P. U., Dyke, A. S., Shakun, J. D., Carlson, A. E., Clark, J., Wohlfarth, B., Mitrovica, J. X., Hostetler, S.  
467 W., and McCabe, A. M.: The Last Glacial Maximum, *Science*, 325, 710–714,  
468 <https://doi.org/10.1126/science.1172873>, 2009.
- 469 Clark, P. U., Shakun, J. D., Baker, P. A., Bartlein, P. J., Brewer, S., Brook, E., Carlson, A. E., Cheng, H., Kaufman,  
470 D. S., Liu, Z., Marchitto, T. M., Mix, A. C., Morrill, C., Otto-Bliesner, B. L., Pahnke, K., Russell, J. M.,  
471 Whitlock, C., Adkins, J. F., Blois, J. L., Clark, J., Colman, S. M., Curry, W. B., Flower, B. P., He, F., Johnson,  
472 T. C., Lynch-Stieglitz, J., Markgraf, V., McManus, J., Mitrovica, J. X., Moreno, P. I., and Williams, J. W.:

- 473 Global climate evolution during the last deglaciation, *PNAS*, 109, E1134–E1142,  
474 <https://doi.org/10.1073/pnas.1116619109>, 2012.
- 475 Cuney, M.: Nuclear geology, in: *Encyclopedia of Geology (Second Edition)*, edited by: Alderton, D. and Elias, S.  
476 A., Academic Press, Cambridge, Massachusetts, United States, 723–744, <https://doi.org/10.1016/B978-0-08-102908-4.00024-2>, 2021.
- 478 Davydova, N. and Servant-Vildary, S.: Late Pleistocene and Holocene history of the lakes in the Kola Peninsula,  
479 Karelia and the North-Western part of the East European plain, *Quat. Sci. Rev.*, 15, 997–1012,  
480 [https://doi.org/10.1016/S0277-3791\(96\)00029-7](https://doi.org/10.1016/S0277-3791(96)00029-7), 1996.
- 481 Fiałkiewicz-koziół, B., Wachniew, P., Woszczyk, M., and Sensuła, B.: High-resolution age-depth model of a peat  
482 bog in Poland as an important basis for paleoenvironmental studies, *Radiocarbon*, 109–125,  
483 <https://doi.org/10.2458/56.16467>, 2014.
- 484 Flantua, S. G. A., Blaauw, M., and Hooghiemstra, H.: Geochronological database and classification system for  
485 age uncertainties in Neotropical pollen records, *Clim. Past*, 12, 387–414, [https://doi.org/10.5194/cp-12-387-](https://doi.org/10.5194/cp-12-387-2016)  
486 2016, 2016.
- 487 Fyfe, R. M., de Beaulieu, J. L., Binney, H., Bradshaw, R. H. W., Brewer, S., Le Flao, A., Finsinger, W., Gaillard,  
488 M. J., Giesecke, T., Gil-Romera, G., Grimm, E. C., Huntley, B., Kunes, P., Köhl, N., Leydet, M., Lotter, A. F.,  
489 Tarasov, P. E., and Tonkov, S.: The European Pollen Database: past efforts and current activities, *Veg. Hist.*  
490 *Archaeobot.*, 18, 417–424, <https://doi.org/10.1007/s00334-009-0215-9>, 2009.
- 491 Gaillard, M. J., Sugita, S., Mazier, F., Trondman, A. K., Broström, A., Hickler, T., Kaplan, J. O., Kjellström, E.,  
492 Kokfelt, U., Kuneš, P., Lemmen, C., Miller, P., Olofsson, J., Poska, A., Rundgren, M., Smith, B., Strandberg,  
493 G., Fyfe, R. M., Nielsen, A. B., Alenius, T., Balakauskas, L., Barnekow, L., Birks, H. J. B., Bjune, A. E.,  
494 Björkman, L., Giesecke, T., Hjelle, K. L., Kalnina, L., Kangur, M., van der Knaap, W. O., Koff, T., Lagerås,  
495 P., Latałowa, M., Leydet, M., Lechterbeck, J., Lindbladh, M., Odgaard, B. V., Peglar, S. M., Segerström, U.,  
496 von Stedingk, H., and Seppä, H.: Holocene land-cover reconstructions for studies on land cover-climate  
497 feedbacks, *Clim. Past*, 6, 483–499, <https://doi.org/10.5194/cp-6-483-2010>, 2010.
- 498 Gajewski, K.: The Global Pollen Database in biogeographical and palaeoclimatic studies, *Prog. Phys. Geog.*, 32,  
499 379–402, <https://doi.org/10.1177/0309133308096029>, 2008.

- 500 [Gajewski, K., Mott, R. J., Ritchie, J. C. and Hadden, K.: Holocene vegetation history of Banks Island, Northwest](#)  
501 [Territories, Canada, \*Can. J. Bot.\*, 78, 430–436, <https://doi.org/10.1139/b00-018>, 2000.](#)
- 502 Giesecke, T., Bennett, K. D., Birks, H. J. B., Bjune, A. E., Bozilova, E., Feurdean, A., Finsinger, W., Froyd, C.,  
503 Pokorný, P., Rösch, M., Seppä, H., Tonkov, S., Valsecchi, V., and Wolters, S.: The pace of Holocene vegetation  
504 change – testing for synchronous developments, *Quat. Sci. Rev.*, 30, 2805–2814,  
505 <https://doi.org/10.1016/j.quascirev.2011.06.014>, 2011.
- 506 Giesecke, T., Davis, B., Brewer, S., Finsinger, W., Wolters, S., Blaauw, M., de Beaulieu, J. L., Binney, H., Fyfe,  
507 R. M., Gaillard, M. J., Gil-Romera, G., van der Knaap, W. O., Kuneš, P., Köhl, N., van Leeuwen, J. F. N.,  
508 Leydet, M., Lotter, A. F., Ortu, E., Semmler, M., and Bradshaw, R. H. W.: Towards mapping the late  
509 Quaternary vegetation change of Europe, *Veg. Hist. Archaeobot.*, 23, 75–86, [https://doi.org/10.1007/s00334-](https://doi.org/10.1007/s00334-012-0390-y)  
510 [012-0390-y](https://doi.org/10.1007/s00334-012-0390-y), 2014.
- 511 Goring, S., Williams, J. W., Blois, J. L., Jackson, S. T., Paciorek, C. J., Booth, R. K., Marlon, J. R., Blaauw, M.,  
512 and Christen, J. A.: Deposition times in the northeastern United States during the Holocene: establishing valid  
513 priors for Bayesian age models, *Quat. Sci. Rev.*, 48, 54–60, <https://doi.org/10.1016/j.quascirev.2012.05.019>,  
514 2012.
- 515 Grigg, L. D. and Whitlock, C.: Patterns and causes of millennial-scale climate change in the Pacific Northwest  
516 during Marine Isotope Stages 2 and 3, *Quat. Sci. Rev.*, 21, 2067–2083, [https://doi.org/10.1016/S0277-](https://doi.org/10.1016/S0277-3791(02)00017-3)  
517 [3791\(02\)00017-3](https://doi.org/10.1016/S0277-3791(02)00017-3), 2002.
- 518 Hajdas, I. and Michczyński, A.: Age-depth model of lake Soppensee (Switzerland) based on the high-resolution  
519 <sup>14</sup>C chronology compared with varve chronology, *Radiocarbon*, 52, 1027–1040,  
520 <https://doi.org/10.1017/S0033822200046117>, 2010.
- 521 Hajdas, I.: Radiocarbon: calibration to absolute time scale, Elsevier, Amsterdam, Netherlands, 14, 37–43,  
522 <https://doi.org/10.1016/B978-0-08-095975-7.01204-3>, 2014.
- 523 [Haslett, J. and Parnell, A.: A simple monotone process with application to radiocarbon-dated depth chronologies, \*J.\*](#)  
524 [R. Stat. Soc. C-Appl., 57, 399-418, <https://doi.org/10.1111/j.1467-9876.2008.00623.x>, 2008.](#)

- 525 [Heaton, T. J., Bard, E., Ramsey, C. B., Butzin, M., Köhler, P., Muscheler, R., Reimer, P. J., and Wacker, L.:](#)  
526 [Radiocarbon: A key tracer for studying Earth's dynamo, climate system, carbon cycle, and Sun, \*Science\*, 374,](#)  
527 [6568, <https://doi.org/10.1126/science.abd7096>, 2021.](#)
- 528 Heaton, T. J., Köhler, P., Butzin, M., Bard, E., Reimer, R. W., Austin, W. E. N., Ramsey, C. B., Grootes, P. M.,  
529 Huguen, K. A., Kromer, B., Reimer, P. J., Adkins, J., Burke, A., Cook, M. S., Olsen, J., and Skinner, L. C.:  
530 Marine20—the marine radiocarbon age calibration curve (0–55,000 cal BP), *Radiocarbon*, 62, 779–820,  
531 <https://doi.org/10.1017/RDC.2020.68>, 2020.
- 532 Herzschuh, U., Boehmer, T., Li, C., Cao, X., Heim, B., and Wiczorek, M.: Global taxonomically harmonized  
533 pollen data collection with revised chronologies, PANGAEA,  
534 <https://doi.pangaea.de/10.1594/PANGAEA.929773>, 2021.
- 535 Herzschuh, U., Cao, X., Laepple, T., Dallmeyer, A., Telford, R. J., Ni, J., Chen, F., Kong, Z., Liu, G., Liu, K.-B.,  
536 Liu, X., Stebich, M., Tang, L., Tian, F., Wang, Y., Wischniewski, J., Xu, Q., Yan, S., Yang, Z., Yu, G., Zhang,  
537 Y., Zhao, Y., and Zheng, Z.: Position and orientation of the westerly jet determined Holocene rainfall patterns  
538 in China, *Nat. Commun.*, 10, 2376, <https://doi.org/10.1038/s41467-019-09866-8>, 2019.
- 539 Hogg, A. G., Heaton, T. J., Hua, Q., Palmer, J. G., Turney, C. S., Southon, J., Bayliss, A., Blackwell, P. G.,  
540 Boswijk, G., Ramsey, C. B., Pearson, C., Petchey, F., Reimer, P., Reimer, R., and Wacker, L.: SHCal20  
541 Southern Hemisphere calibration, 0–55,000 years cal BP, *Radiocarbon*, 62, 759–778,  
542 <https://doi.org/10.1017/RDC.2020.59>, 2020.
- 543 Hua, Q., Barbetti, M., and Rakowski, A. Z.: Atmospheric radiocarbon for the period 1950–2010, *Radiocarbon*,  
544 55, 2059–2072, [https://doi.org/10.2458/azu\\_js\\_rc.v55i2.16177](https://doi.org/10.2458/azu_js_rc.v55i2.16177), 2013.
- 545 Jennerjahn, T. C., Ittekkot, V., Arz, H. W., Behling, H., Pätzold, J., and Wefer, G.: Asynchronous terrestrial and  
546 marine signals of climate change during Heinrich events, *Science*, 306, 2236–2239,  
547 <https://doi.org/10.1126/science.1102490>, 2004.
- 548 Lane, C. S., Blockley, S. P. E., Mangerud, J., Smith, V. C., Lohne, Ø. S., Tomlinson, E. L., Matthews, I. P., and  
549 Lotter, A. F.: Was the 12.1ka Icelandic Vedde Ash one of a kind?, *Quat. Sci. Rev.*, 33, 87–99,  
550 <https://doi.org/10.1016/j.quascirev.2011.11.011>, 2012.

- 551 Li, C., Postl, A., Boehmer, T., Dolman, A. M., and Herzschuh, U.: Harmonized chronologies of a global late  
552 Quaternary pollen dataset (LegacyAge 1.0), PANGAEA, <https://doi.pangaea.de/10.1594/PANGAEA.933132>,  
553 [2021](https://doi.pangaea.de/10.1594/PANGAEA.933132).
- 554 [Li, C., Postl, A., Boehmer, T., Dolman, A. M., and Herzschuh, U.: Harmonized chronologies of a global late](https://doi.org/10.5281/zenodo.5815192)  
555 [Quaternary pollen dataset \(LegacyAge 1.0\) in R, Zenodo, https://doi.org/10.5281/zenodo.5815192, 2022.](https://doi.org/10.5281/zenodo.5815192)
- 556 Lowe, D. J.: Tephrochronology and its application: A review, *Quat. Geochronol.*, 6, 107–153,  
557 <https://doi.org/10.1016/j.quageo.2010.08.003>, 2011.
- 558 [Marsicek, J., Shuman, B. N., Bartlein, P. J., Shafer, S. L. and Brewer, S.: Reconciling divergent trends and](https://doi.org/10.1038/nature25464)  
559 [millennial variations in Holocene temperatures, \*Nature\*, 554, 92-96, https://doi.org/10.1038/nature25464, 2018.](https://doi.org/10.1038/nature25464)
- 560 [Mauri, A., Davis, B. A. S., Collins, P. M. and Kaplan, J. O.: The climate of Europe during the Holocene: a gridded](https://doi.org/10.1016/j.quascirev.2015.01.013)  
561 [pollen-based reconstruction and its multi-proxy evaluation, \*Quat. Sci. Rev.\*, 112, 109-127,](https://doi.org/10.1016/j.quascirev.2015.01.013)  
562 [https://doi.org/10.1016/j.quascirev.2015.01.013, 2015.](https://doi.org/10.1016/j.quascirev.2015.01.013)
- 563 Mottl, O., Flantua, S. G. A., Bhatta, K. P., Felde, V. A., Giesecke, T., Goring, S., Grimm, E. C., Haberle, S.,  
564 Hooghiemstra, H., Ivory, S., Kuneš, P., Wolters, S., Seddon, A. W. R., and Williams, J. W.: Global acceleration  
565 in rates of vegetation change over the past 18,000 years, *Science*, 372, 860–864,  
566 <https://doi.org/10.1126/science.abg1685>, 2021.
- 567 Niemann, H. and Behling, H.: Late Quaternary vegetation, climate and fire dynamics inferred from the El Tiro  
568 record in the southeastern Ecuadorian Andes, *J. Quat. Sci.*, 23, 203–212, <https://doi.org/10.1002/jqs.1134>, 2008.
- 569 Ojala, A. E. K., Francus, P., Zolitschka, B., Besonen, M., and Lamoureux, S. F.: Characteristics of sedimentary  
570 varve chronologies – A review, *Quat. Sci. Rev.*, 43, 45–60, <https://doi.org/10.1016/j.quascirev.2012.04.006>,  
571 2012.
- 572 Philippsen, B. and Heinemeier, J.: Freshwater reservoir effect variability in northern Germany, *Radiocarbon*, 55,  
573 1085–1101, <https://doi.org/10.1017/S0033822200048001>, 2013.
- 574 Philippsen, B.: The freshwater reservoir effect in radiocarbon dating, *Herit. Sci.*, 1, 24,  
575 <https://doi.org/10.1186/2050-7445-1-24>, 2013.

- 576 R Core Team: R: A language and environment for statistical computing, R Foundation for Statistical Computing,  
577 Vienna, Austria, 2021.
- 578 Ramisch, A., Brauser, A., Dorn, M., Blanchet, C., Brademann, B., Köppl, M., Mingram, J., Neugebauer, I.,  
579 Nowaczyk, N., Ott, F., Pinkerneil, S., Plessen, B., Schwab, M. J., Tjallingii, R., and Brauer, A.: VARDA  
580 (VARved sediments DAtabase) – providing and connecting proxy data from annually laminated lake sediments,  
581 Earth Syst. Sci. Data, 12, 2311–2332, <https://doi.org/10.5194/essd-12-2311-2020>, 2020.
- 582 [Ramsey, C. B.: Deposition models for chronological records, Quat. Sci. Rev., 27, 42–60,](https://doi.org/10.1016/j.quascirev.2007.01.019)  
583 <https://doi.org/10.1016/j.quascirev.2007.01.019>, 2008.
- 584 Rasmussen, S. O., Bigler, M., Blockley, S. P., Blunier, T., Buchardt, S. L., Clausen, H. B., Cvijanovic, I., Dahl-  
585 Jensen, D., Johnsen, S. J., Fischer, H., Gkinis, V., Guillevic, M., Hoek, W. Z., Lowe, J. J., Pedro, J. B., Popp,  
586 T., Seierstad, I. K., Steffensen, J. P., Svensson, A. M., Vallelonga, P., Vinther, B. M., Walker, M. J. C.,  
587 Wheatley, J. J., and Winstrup, M.: A stratigraphic framework for abrupt climatic changes during the Last  
588 Glacial period based on three synchronized Greenland ice-core records: refining and extending the INTIMATE  
589 event stratigraphy, Quat. Sci. Rev., 106, 14–28, <https://doi.org/10.1016/j.quascirev.2014.09.007>, 2014.
- 590 Reimer, P. J., Austin, W. E. N., Bard, E., Bayliss, A., Blackwell, P. G., Ramsey, C. B., Butzin, M., Cheng, H.,  
591 Edwards, R. L., Friedrich, M., Grootes, P. M., Guilderson, T. P., Hajdas, I., Heaton, T. J., Hogg, A. G., Hughen,  
592 K. A., Kromer, B., Manning, S. W., Muscheler, R., Palmer, J. G., Pearson, C., van der Plicht, J., Reimer, R. W.,  
593 Richards, D. A., Scott, E. M., Southon, J. R., Turney, C. S. M., Wacker, L., Adolphi, F., Büntgen, U., Capano,  
594 M., Fahrni, S. M., Fogtmann-Schulz, A., Friedrich, R., Köhler, P., Kudsk, S., Miyake, F., Olsen, J., Reinig, F.,  
595 Sakamoto, M., Sookdeo, A., and Talamo, S.: The IntCal20 Northern Hemisphere radiocarbon age calibration  
596 curve (0–55 cal kBP), Radiocarbon, 62, 725–757, <https://doi.org/10.1017/RDC.2020.41>, 2020.
- 597 Roberts, N.: The Holocene: An Environmental History (third edition), John Wiley & Sons, Chichester, UK, 415  
598 pp., 2013.
- 599 Sánchez Goñi, M. F., Desprat, S., Daniau, A. L., Bassinot, F. C., Polanco-Martínez, J. M., Harrison, S. P., Allen,  
600 J. R. M., Anderson, R. S., Behling, H., Bonnefille, R., Burjachs, F., Carrión, J. S., Cheddadi, R., Clark, J. S.,  
601 Combourieu-Nebout, N., Mustaphi, C. J. C., Debusk, G. H., Dupont, L. M., Finch, J. M., Fletcher, W. J.,  
602 Giardini, M., González, C., Gosling, W. D., Grigg, L. D., Grimm, E. C., Hayashi, R., Helmens, K., Heusser, L.

- 603 E., Hill, T., Hope, G., Huntley, B., Igarashi, Y., Irino, T., Jacobs, B., Jiménez-Moreno, G., Kawai, S., Kershaw,  
604 A. P., Kumon, F., Lawson, I. T., Ledru, M. P., Lézine, A. M., Liew, P. M., Magri, D., Marchant, R., Margari,  
605 V., Mayle, F. E., McKenzie, G. M., Moss, P., Müller, S., Müller, U. C., Naughton, F., Newnham, R. M., Oba,  
606 T., Pérez-Obiol, R., Pini, R., Ravazzi, C., Roucoux, K. H., Rucina, S. M., Scott, L., Takahara, H., Tzedakis, P.  
607 C., Urrego, D. H., van Geel, B., Valencia, B. G., Vandergoes, M. J., Vincens, A., Whitlock, C. L., Willard, D.  
608 A., and Yamamoto, M.: The ACER pollen and charcoal database: a global resource to document vegetation and  
609 fire response to abrupt climate changes during the last glacial period, *Earth Syst. Sci. Data*, 9, 679–695,  
610 <https://doi.org/10.5194/essd-9-679-2017>, 2017.
- 611 Trachsel, M. and Telford, R. J.: All age-depth models are wrong, but are getting better, *The Holocene*, 27, 860–  
612 869, <https://doi.org/10.1177/0959683616675939>, 2017.
- 613 Trondman, A. K., Gaillard, M. J., Mazier, F., Sugita, S., Fyfe, R. M., Nielsen, A. B., Twiddle, C., Barratt, P.,  
614 Birks, H. J. B., Bjune, A. E., Björkman, L., Broström, A., Caseldine, C., David, R., Dodson, J., Dörfler, W.,  
615 Fischer, E., van Geel, B., Giesecke, T., Hultberg, T., Kalnina, L., Kangur, M., van der Knaap, W. O., Koff, T.,  
616 Kuneš, P., Lagerås, P., Latałowa, M., Lechterbeck, J., Leroyer, C., Leydet, M., Lindbladh, M., Marquer, L.,  
617 Mitchell, F. J. G., Odgaard, B. V., Peglar, S. M., Persson, T., Poska, A., Rösch, M., Seppä, H., Veski, S., and  
618 Wick, L.: Pollen-based quantitative reconstructions of Holocene regional vegetation cover (plant-functional  
619 types and land-cover types) in Europe suitable for climate modelling, *Global Change Biol.*, 21, 676–697,  
620 <https://doi.org/10.1111/gcb.12737>, 2015.
- 621 Wallinga, J. and Cunningham, A. C.: Luminescence dating, uncertainties and age range, In *Encyclopedia of*  
622 *Scientific Dating Methods*, Springer, Dordrecht, Netherlands, 440-445, 2015.
- 623 Wang, J., Zhu, L., Wang, Y., Peng, P., Ma, Q., Haberzettl, T., Kasper, T., Matsunaka, T., and Nakamura, T.:  
624 Variability of the  $^{14}\text{C}$  reservoir effects in Lake Tangra Yumco, Central Tibet (China), determined from recent  
625 sedimentation rates and dating of plant fossils, *Quat. Int.*, 430, 3–11,  
626 <https://doi.org/10.1016/j.quaint.2015.10.084>, 2017.
- 627 Wang, Y., Goring, S. J. and McGuire, J. L.: Bayesian ages for pollen records since the last glaciation in North  
628 America, *Sci. Data*, 6, 176, <https://doi.org/10.1038/s41597-019-0182-7>, 2019.

- 629 Williams, J. W., Grimm, E. C., Blois, J. L., Charles, D. F., Davis, E. B., Goring, S. J., Graham, R. W., Smith, A.  
630 J., Anderson, M., Arroyo-Cabrales, J., Ashworth, A. C., Betancourt, J. L., Bills, B. W., Booth, R. K., Buckland,  
631 P. I., Curry, B. B., Giesecke, T., Jackson, S. T., Latorre, C., Nichols, J., Purdum, T., Roth, R. E., Stryker, M.,  
632 and Takahara, H.: The Neotoma Paleoecology Database, a multiproxy, international, community-curated data  
633 resource, *Quat. Res.*, 89, 156–177, <https://doi.org/10.1017/qua.2017.105>, 2018.
- 634 Zolitschka, B., Francus, P., Ojala, A. E. K., and Schimmelmann, A.: Varves in lake sediments – a review, *Quat.*  
635 *Sci. Rev.*, 117, 1–41, <https://doi.org/10.1016/j.quascirev.2015.03.019>, 2015.